Bootstrapped gross error detection for efficient and fault-tolerant real-time optimization

Gabriel D. Patrón,[1] Luis Ricardez-Sandoval[1]

***Abstract*— Real-time optimization (RTO) is a model-based approach for generating economically optimal steady-state process set points. The process model used in RTO requires reconciliation with the plant through parameter estimation, which uses online measurements. In the presence of sensor faults causing measurement bias, the estimation layer can result in suboptimal set points that may violate safety, environmental, or operational constraints. Herein, a gross error detection approach is proposed to determine measurement sets that exclude faults, thus avoiding estimation errors propagating to the set points and ensuring safe operation. This is achieved by computing parameter estimate samples offline using varying measurement combinations and bootstrapping available plant data. The resulting parameter estimates are subjected to single-sample t-tests to determine which estimates are significantly different; these correspond to the measurement that have the highest probability of being faulty. The computational complexity of the algorithm is discussed, whereby it is shown to be related to the observability criteria and number of measurements. A continuously stirred tank reactor with an upper bound on heat generation is used to exemplify the proposed approach in a process safety setting. The incidence of constraint-violating operation is observed to decrease in both frequency and severity when using the proposed framework; thus, the resulting set points are economical while ensuring safe heating limits are respected during operation.**

I. Introduction

In increasingly competitive production environments, the model-based economic optimization of process systems can provide competitive advantages to operators. Real-time optimization (RTO) has emerged as the foremost option for economic optimization in both academia and industry [1] with applications in fuel cells [2], polymerization [3], and carbon capture [4]. RTO uses a steady-state process model to generate set points that a control layer can track; these are updated periodically or upon the detection of disturbances. Highly detailed mechanistic models are typically used in RTO; despite this, simplifying assumptions must be made such that models can be evaluated by conventional optimization solvers. These model simplifications lead to plant-model mismatch, which must be addressed by adapting the model within the RTO procedure to reconcile it with the plant. Two adaptation strategies are common in RTO: the "two-step" procedure for parametric uncertainty [5] and the "modifier adaptation" procedure for structural uncertainty; the former is more commonly used and is the topic of the present study, the reader is referred to [6] for information on the latter. In cases of parametric mismatch when the two-step RTO procedure is used, a parameter estimation (PE) layer uses steady-state measurements to update the model prior to solving the economic optimization problem. On a shorter timescale, the process controller regulates the plant towards the RTO-supplied set points. This procedure is depicted in Fig.1.

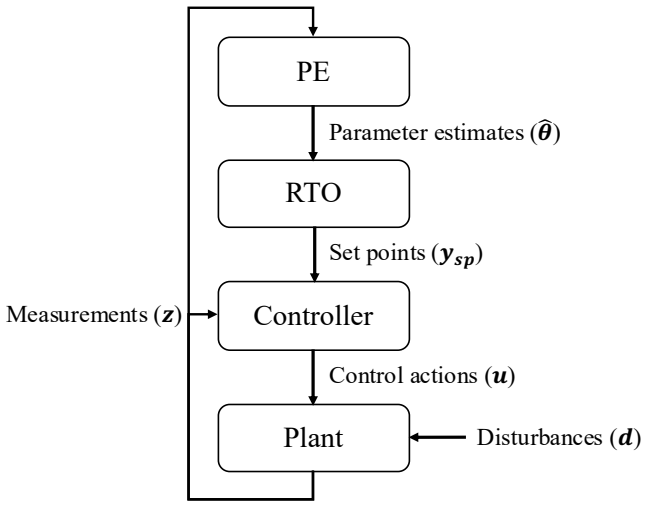

Figure 1. Typical two-step RTO procedure.

The typical RTO architecture is crucially reliant on the measurements acquired from the plant, making it vulnerable to noise and faults (i.e., random and systematic errors). The propagation of these errors to the PE layer, and subsequently to the set points, can cause economic suboptimalities as well as constraint violations. In the latter case, constraints can include safety requirements that ensure the continued operation and well-being of plant operators and equipment; violating these constraints can have severe consequences such as injury or equipment damage, respectively.

A few techniques have been proposed to abate the effect of these errors (robust estimators) and identify where they occur (gross error detection, GED). Generally, hypothesis testing is used for identifying measurements containing gross errors. This requires a measurement baseline in which no gross error is present [7] along with constant observation of measurements to capture potential drift. More recent approaches have used optimal data reconciliation to ensure measurements are consistent with the model before being used for PE [8]. The use of robust estimators (e.g., [8]) abates the effect of measurement bias on parameters; however, they do not identify where a fault is located, nor do they fully eliminate its effects. Moreover, the modified iterative measurement test (MIMT) [9] uses residuals from a least-squares data reconciliation procedure along with statistical hypothesis

* The authors would like to acknowledge the Natural Sciences and Engineering Research Council of Canada (NSERC) for their financial support.

[1]University of Waterloo, Department of Chemical Engineering, Waterloo, ON, N2L 3G1, Canada (Tel: +1 (519)-888-4567 ex:38667; e-mail: laricard@uwaterloo.ca).

testing to sequentially eliminate outlier estimates; however, this method requires local linearized constraints to be estimated to generate a residual covariance matrix.

The work presented herein builds on the existing GED literature by proposing a new scheme that leverages modern computational power and is readily retrofitted into existing RTO systems (i.e., no additional experiments, layers, or samples are necessary). We propose constructing bootstrapped parameter estimate samples that can be used for determining measurement subsets that lead to significant differences in parameter estimates, thus are likely to contain gross errors. In contrast to previously GED schemes, the present work takes a parameter-driven approach to identifying faults. That is, faults are not detected until they significantly propagate to the parameter estimates (and resultantly, the set points). The focus on parameters constitutes a novelty in the process GED literature where the effect of the faults on plant optimality are prioritized through economics and constraints. Such an emphasis on constraints is crucial in processes where safe operation must be ensured.

This study is structured as follows: section II outlines the standard two-step RTO formulations; section III details and discusses the bootstrapped GED method; section IV provides a CSTR case study that compares the performance of the proposed scheme against the traditional RTO in a safety-constrained setting; section V summarizes key findings from this work.

II. Two-step RTO Formulations

A. Preliminaries

Scalar quantities are denoted as *unbolded* while vector/matrix quantities are ***bolded***. $\|\boldsymbol{a}\|_{\boldsymbol{B}}{}^2$ denotes a quadratic form on an n-dimensional vector $\boldsymbol{a} \in \mathbb{R}^n$ with an $(n \times n)$-dimensional weighting matrix $\boldsymbol{B} \in \mathbb{R}^{n \times n}$. $\|\boldsymbol{a}\|_\infty$ denotes the infinity-norm (i.e., maximum norm) on a vector. $\{\boldsymbol{a_t}\}_{t=1}^T$ denotes a sample of T observations of vector $\boldsymbol{a}$ acquired over the sampling periods $t \in \{\mathbb{Z} | 1 \leq t \leq T\}$. $\bar{\boldsymbol{a}}$ denotes the sample-averaged mean of $\{\boldsymbol{a_t}\}_{t=1}^T$ (i.e., $\bar{\boldsymbol{a}} = \frac{1}{T}\sum_{t=1}^T \boldsymbol{a_t}$). The sample vector covariance matrix ($\boldsymbol{Q_a} \in \mathbb{R}^{n \times n}$) has elements computed as $Q_{i,j,a} = \frac{1}{T}\sum_{t=1}^T (a_{i,t} - \bar{a}_i)(a_{j,t} - \bar{a}_j)$ where $a_{i,t}$ and $a_{j,t}$ are the i^{th} and j^{th} components of $\boldsymbol{a}$.

Sets are denoted in script (e.g., $\mathcal{M}$). $\mathcal{P}(\mathcal{M})$ denotes the power set of $\mathcal{M}$ while $\mathcal{S} = \mathcal{P}_K(\mathcal{M})$ denotes the subsets of the power set of $\mathcal{M}$ with cardinality K. $\mathcal{S}_j = \{\mathcal{S} | j \in \mathcal{S}\}$ denotes the subsets of $\mathcal{S}$ that contain the element j. This set notation is used for denoting measurements and operations on measurements; an example is shown in Fig. 2 for clarity. \ denotes the set difference, i.e. $\mathcal{M} \backslash j = \{\mathcal{M} | j \notin \mathcal{M}\}$.

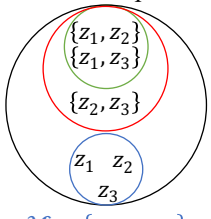

$\mathcal{M} = \{z_1, z_2, z_3\}$

$\mathcal{P}(\mathcal{M}) = \{\{\,\}, \{z_1\}, \{z_2\}, \{z_3\}, \{z_1, z_2\}, \{z_1, z_3\}, \{z_2, z_3\}, \{z_1, z_2, z_3\}\}$

$\mathcal{S} = \mathcal{P}_2(\mathcal{M}) = \{\{z_1, z_2\}, \{z_1, z_3\}, \{z_2, z_3\}\}$

$\mathcal{S}_{z_1} = \{\{z_1, z_2\}, \{z_1, z_3\}\}$

Figure 2. Example of three-measurement set and associated operations.

B. Economic Optimization Layer

The steady-state economic optimization problem used within the two-layer RTO scheme is posed as follows:

$$\begin{aligned} &\min_{\boldsymbol{y_{sp}} = \hat{\boldsymbol{y}}} \phi(\hat{\boldsymbol{x}}) \\ &s.t. \\ &\boldsymbol{f}(\boldsymbol{d}, \boldsymbol{u}, \hat{\boldsymbol{x}}, \hat{\boldsymbol{y}}, \hat{\boldsymbol{\theta}}) = 0 \\ &\boldsymbol{g}(\boldsymbol{d}, \boldsymbol{u}, \hat{\boldsymbol{x}}) \leq 0 \\ &\boldsymbol{u} \in \boldsymbol{\mathcal{U}} \\ &\boldsymbol{y} \in \boldsymbol{\mathcal{Y}} \end{aligned} \tag{1}$$

where $\phi: \mathbb{R}^{n_x} \to \mathbb{R}$ is an economic objective to be optimized (cost minimization is taken as the standard convention). The process economic objective maps the model-predicted process states $\hat{\boldsymbol{x}} \in \mathbb{R}^{n_x}$ to a scalar cost function. The economic objective is subject to the steady-state model $\boldsymbol{f}: \mathbb{R}^{n_d} \times \mathbb{R}^{n_u} \times \mathbb{R}^{n_\theta} \to \mathbb{R}^{n_x} \times \mathbb{R}^{n_y}$, which maps the process disturbances $\boldsymbol{d} \in \mathbb{R}^{n_d}$, inputs $\boldsymbol{u} \in \mathbb{R}^{n_u}$, and model parameters $\hat{\boldsymbol{\theta}} \in \mathbb{R}^{n_\theta}$ to the predicted states and controlled variables $\hat{\boldsymbol{y}} \in \mathbb{R}^{n_y}$ of the system. The economically optimal controlled variables are the decision variables for the RTO problem, whereby they are passed to the control layer as set points ($\boldsymbol{y_{sp}} = \hat{\boldsymbol{y}}$). Accordingly, the controlled variables and their corresponding manipulated variables are bounded within the user-defined feasible regions $\boldsymbol{\mathcal{Y}}$ and $\boldsymbol{\mathcal{U}}$, respectively. In addition to the bounds, the RTO can also be given additional constraints $\boldsymbol{g}: \mathbb{R}^{n_d} \times \mathbb{R}^{n_u} \times \mathbb{R}^{n_x} \to \mathbb{R}^{n_g}$; these can include safety or quality constraints. The quality of the model predictions, thus the fidelity of the RTO-defined set points to the true plant optima, and the adherence to constraints, are dependent on $\hat{\boldsymbol{\theta}}$.

C. Parameter Adaptation Layer

To ensure good agreement with the plant, a PE problem is executed to update the RTO model prior to finding an economic solution. The PE problem is posed as follows:

$$\begin{aligned} &\min_{\hat{\boldsymbol{\theta}}} \|\hat{\boldsymbol{z}} - \bar{\boldsymbol{z}}\|_{\boldsymbol{Q_z}^{-1}}{}^2 \\ &\boldsymbol{f}(\boldsymbol{d}, \boldsymbol{u}, \hat{\boldsymbol{x}}, \hat{\boldsymbol{y}}, \hat{\boldsymbol{\theta}}) = \boldsymbol{0} \\ &\boldsymbol{h}(\hat{\boldsymbol{x}}) = \hat{\boldsymbol{z}} \\ &\hat{\boldsymbol{\theta}} \in \boldsymbol{\Theta} \end{aligned} \tag{2}$$

where all variables are defined as in (1). Additionally, an observation model $\boldsymbol{h}: \mathbb{R}^{n_x} \to \mathbb{R}^{n_z}$ maps the model-predicted states to measurement predictions $\hat{\boldsymbol{z}} \in \mathbb{R}^{n_z}$ and the feasible region $\boldsymbol{\Theta}$ is defined for the model parameters, which are the decision variables for the PE problem. The objective function in (2) minimizes the difference between the sample-averaged steady-state measurements and the model measurement predictions such that the plant and model are reconciled through the parameters estimates.

III. Bootstrapped Gross Error Detection

A gross error detection approach is proposed, whereby the measurement exclusion [10] and data bootstrapping principles [11] are extended to an RTO and GED context using a novel parameter hypothesis testing approach. The proposed scheme creates parameter samples through measurement exclusion,

from which measurements that result in statistically erroneous parameters can be identified. By applying a parameter-driven technique to GED, the aim of the proposed algorithm is to ensure optimal and safe RTO performance. The scheme makes the following assumptions:

1. The measurement noise is Gaussian, which is necessary condition for the least-squares estimation formulation presented in (2).
2. The plant Karush-Kuhn-Tucker (KKT) conditions can be fulfilled by the joint PE/RTO procedure [5].
3. The faults manifest through a recurring measurement bias.

A. Bootstrapping Available Data

The proposed scheme is designed for retrofitting existing RTO systems. Accordingly, it is assumed that the steady-state sample size is defined for the existing RTO *a priori* as M. With M observations, M parameter estimates (i.e., $\{\widehat{\boldsymbol{\theta}}_{\boldsymbol{t}}\}_{t=1}^{M}$) can be generated by re-sampling and using $M-1$ measurements in the RTO averaging procedure (i.e., calculation of $\bar{\boldsymbol{z}}$ and $\boldsymbol{Q_z}$). Each estimate is generated by removing a single observation and resampling the remaining $M-1$ points. As shown in Fig. 3, each colour represents a different measurement sample. The blue sample generates $\widehat{\boldsymbol{\theta}}_{\boldsymbol{t=1}}$ by excluding the sample point $\boldsymbol{z}_{\boldsymbol{t=1}}$, and the red sample generates $\widehat{\boldsymbol{\theta}}_{\boldsymbol{t=2}}$ by excluding $\boldsymbol{z}_{\boldsymbol{t=2}}$; this exclusion and re-sampling procedure is repeated until $\{\widehat{\boldsymbol{\theta}}_{\boldsymbol{t}}\}_{t=1}^{M}$ is completed with the green sample that excludes $\boldsymbol{z}_{\boldsymbol{t=M}}$. By following this procedure, estimate statistics can be constructed such that hypothesis testing can be applied to the estimate sample.

B. Identifying Faults

The bootstrapped parameter estimate procedure is applied to various measurement sets. Given the complete set of measurement $\mathcal{M} = \{z_1, \dots, z_{n_z}\}$, a given number (n_K) of subsets with cardinality K are possible to construct. Partial measurement vectors are accordingly defined as $\boldsymbol{\zeta_i} \in \mathbb{R}^K$ where $i \in \mathcal{S}$ and $\mathcal{S} = \mathcal{P}_K(\mathcal{M})$ as defined previously. Each partial measurement vector, and their corresponding steady-state samples $\{\boldsymbol{\zeta_{i_t}}\}_{t=1}^{M}$, are used to generate estimate samples $\{\widehat{\boldsymbol{\theta}}_{\boldsymbol{i_t}}\}_{t=1}^{M}$ following the boostrapping procedure outlined in the previous section. From these, sample-averaged parameter means for each measurement subset are computed (i.e., $\overline{\boldsymbol{\theta}}_{\boldsymbol{i}}$).

For $\overline{\boldsymbol{\theta}}_{\boldsymbol{i}}\ \forall i \in \mathcal{S}$, the following single-sample hypothesis test is performed:

$$\begin{aligned} H_0&: \overline{\boldsymbol{\theta}} = \overline{\boldsymbol{\theta}}_{\boldsymbol{i}} \\ H_1&: \overline{\boldsymbol{\theta}} \neq \overline{\boldsymbol{\theta}}_{\boldsymbol{i}} \end{aligned} \tag{3}$$

where $\overline{\boldsymbol{\theta}} = \frac{1}{n_K}\sum_{i\in S}\overline{\boldsymbol{\theta}}_{\boldsymbol{i}}$ are the measurement subset-averaged parameter values. The null hypothesis assumes that each individual sample-averaged parameter is equivalent to the measurement subset-averaged parameter; this would be the case if a fault were not contained within the tested measurement set as it would not propagate to the estimates. The alternative hypothesis accounts for potential differences in sample-averaged parameters and measurement subset-averaged parameters; this indicates that a fault is present and therefore would propagate to the RTO. Each hypothesis test generates a two-sided t-test p-value for its corresponding measurement set and model parameters. The vectors $\boldsymbol{P_i} \in \mathbb{R}^{n_\theta}\ \forall i \in \mathcal{S}$ contain the p-values associated with the samples of n_θ parameter estimates, which are generated using bootstrapped samples of the partial measurement set i. These p-values determine whether parameters generated by a given measurement set are within the true parameter distribution given a chosen significance level α, which is the critical value for the hypothesis test.

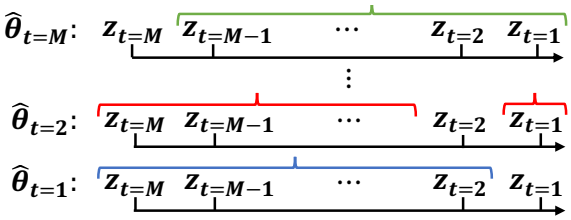

Figure 3. Parameter estimate bootstrapping.

A single parameter estimate generated using an arbitrary measurement set i is identified as erroneous if $P_{i,\theta} < \alpha$. This is extended to multi-parameter systems by imposing the condition that a vector of parameters is identified as erroneous if any parameter within it is erroneous. Moreover, this criterion must apply for cases with many measurements $\mathcal{M}$. For a measurement to be deemed erroneous, all partial measurement subsets containing the measurement j (i.e., $\mathcal{S}_j$) must fulfill the alternative hypothesis. Accordingly, in a multi-parameter and multi-measurement setting, H_0 is rejected if the following condition holds:

$$\|-\boldsymbol{P_i}\|_\infty > -\alpha, \qquad \forall i \in \mathcal{S}_j \tag{4}$$

such that the measurement j contains the fault as identified in its parameter estimates. The negative of the maximum norm finds the minimum element in the vector $\boldsymbol{P_i}$ and the inequality identifies whether the minimum element is smaller than the significance threshold α (i.e., the minimum element is larger than $-\alpha$). Accordingly, a single parameter from the parameter vector corresponding to each member of $\mathcal{S}_j$ must be identified as erroneous for a fault to be detected.

If criterion (4) is fulfilled, then it is used sequentially on the measurements within $\mathcal{M}$ whereby the measurement j that has the highest probability of being erroneous (i.e., smallest p-value/largest negative p-value) is removed, i.e.:

$$j = argmax\{\|-\boldsymbol{P_i}\|_\infty | \forall i \in \mathcal{S}_j | \forall j \in \mathcal{M}\} \tag{5}$$

Once j is identified, it is removed from the measurement set thereafter (i.e., $\mathcal{M} \leftarrow \mathcal{M}\backslash j$) and the hypothesis testing procedure is repeated by calculating a new subset-averaged parameter mean ($\overline{\boldsymbol{\theta}}$) excluding j. This continues until criterion (4) is no longer fulfilled, thus there are no remaining faults that propagate to the parameter estimates since all measurement combinations yield statistically similar parameters. This is a key difference in the present bootstrapped GED with respect to past GED schemes; since the hypothesis testing is parameter-driven, faults are not identified unless they have a significant effect on the RTO through the parameter estimates.

The algorithm proposed in this work is summarized in Fig. 4. Firstly, the acquired measurement sample is used for the

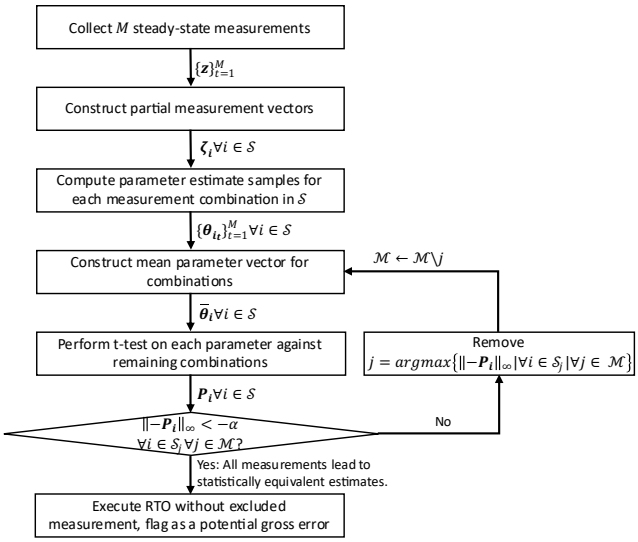

Figure 4. Bootstrapped RTO+GED algorithm.

bootstrapping procedure to generate parameter estimate samples assuming different measurement subsets in $\mathcal{S}$. Secondly, the measurement subset generated parameter samples $\{\widehat{\boldsymbol{\theta}}_{\boldsymbol{it}}\}_{t=1}^{M}$ undergo hypothesis testing with respect to the subset-averaged parameter means $\bar{\boldsymbol{\theta}}$. If all measurement subsets containing a given measurement type are found to be significantly different, then that measurement type is flagged as faulty and excluded from the RTO procedure. This is repeated until all measurement subsets are found to yield statistically similar parameters at which point, lastly, the RTO is computed with the faultless measurements.

C. Computational Complexity

The size of measurement set is determined by the observability criteria of the system whereby $n_{z,min}$ is the *a priori* determined minimum number of measurements to retain parameter observability. The observability requirement has the corollary that $n_z > n_{z,min}$ for the proposed approach to be deployed (i.e., at least one measurement can be excluded). Accordingly, in a system with n_z sensors, n_z choose $n_{z,min}$ combinations can be used to generate parameter estimates, i.e.:

$$n_K(n_z, n_{z,min}) = \frac{n_z!}{n_{z,min}!\,(n_z - n_{z,min})!} \tag{6}$$

We define $K = n_{z,min}$ from section III*B* such that the number of subsets of $n_{z,min}$ cardinality to ensure that the algorithm defined in the previous section ensures observability is n_K as per (6). The bootstrapping procedure thus requires $n_{PE} = n_K \times M$ parameter estimation problems to be solved. Accordingly, the computational effort scales factorially with the number of measurements and inversely factorial with the observability requirements. The number of measurements thus determines the dominant computational cost of the proposed scheme as the hypothesis testing time is negligible in comparison to the bootstrap time. For many cases $n_{z,min} = n_\theta$ is required for observability. However, for situations with many measurements, $n_{z,min}$ can be assumed to be higher than that needed for observability; this could decrease the computational effort required at the expense of fault specificity (i.e., measurements would have to be lumped into groups).

IV. CSTR Case Study

A. CSTR Model

The proposed approach is deployed on a two-reaction CSTR [12], where feeds of reactants A and B generate C with D as a byproduct. The system is modelled as follows:

$$\frac{dC_A}{dt} = -k_1 C_A C_B + \frac{u_A}{V} C_{A,in} - \left(\frac{u_A + u_B}{V}\right) C_A \tag{7}$$

$$\frac{dC_B}{dt} = -k_1 C_A C_B - 2k_2 {C_B}^2 + \frac{u_B}{V} C_{B,in} - \left(\frac{u_A + u_B}{V}\right) C_B \tag{8}$$

$$\frac{dC_C}{dt} = k_1 C_A C_B - \left(\frac{u_A + u_B}{V}\right) C_C \tag{9}$$

$$\frac{dC_D}{dt} = k_2 {C_B}^2 - \left(\frac{u_A + u_B}{V}\right) C_D \tag{10}$$

$$Q = V k_1 C_A C_B (-\Delta H_{r,1}) + V k_2 {C_B}^2 (-\Delta H_{r,2}) \tag{11}$$

$$D = \frac{C_D}{C_A + C_B + C_C + C_D} \tag{12}$$

where C_A, C_B, C_C, and $C_D (mol/L)$ denote the concentrations of the constituent species. $Q(kcal/min)$ and $D(mol/mol)$ denote the heat generated by the reactions and the selectivity to species D, respectively. u_A and $u_B (L/min)$ denote the feed flowrates, which are the process manipulated variables. $C_{A,in} = 2$ and $C_{B,in} = 1.5\ mol/L$ are the inlet concentrations of feeds. $k_1 = 0.75$ and $k_2 = 1.5\ L/(mol \cdot min)$ are the reaction rate constants, while $\left(-\Delta H_{r,1}\right) = 3.5$ and $\left(-\Delta H_{r,2}\right) = 1.5\ kcal/mol$ are the reaction enthalpies. $V = 500\ L$ is the reactor volume.

B. CSTR Economic Optimization Formulation

The model described by (7)–(12) is used to represent the steady-state plant and deployed as $\boldsymbol{f}$ for the RTO problem (1). The following constraints ($\boldsymbol{g}$) are imposed on the RTO:

$$Q \leq Q_{max} \tag{13}$$

$$D \leq D_{max} \tag{14}$$

where Q_{max} and D_{max} are maximal heat generation and selectivity, respectively. While (13) is related to safety, (14) is a product quality (i.e., purity) constraint; both aspects of operation must be fulfilled to continually generate a commercially viable product from this process. While a below-grade product is undesirable, it may be re-processed; however, unsafe operation can have lasting effects ranging from lost productivity in the event of a shutdown to injury in the event of operator exposure. Thus, it is crucial to satisfy this heating constraint to avoid long-term losses.

The manipulated variables (feed flowrates) are constrained as $\boldsymbol{U} = \{(u_A, u_B) | 0 \leq u_A, u_B \leq u_{max}\}$. Perfect control is assumed (i.e., the set points can be reached by the control layer); thus, the manipulated variable bounds serve to construct the feasible region for the RTO problem. An objective function that maximizes productivity of product C while minimizing the control effort is considered; this is expressed as follows:

$$-\phi = \frac{{C_C}^2(u_A + u_B)^2}{u_A C_{A,in}} - w({u_A}^2 + {u_B}^2) \quad (15)$$

where w is a penalty weight. Note that the LHS of (15) uses a negative sign to convert the maximization to minimization; this keeps consistency with (1). The optimization parameters are [12]: $w = 0.004\ (mol \cdot min)/L^2$, $Q_{max} = 110\ kcal/min$, $D_{max} = 0.1\ mol/mol$, and $u_{max} = 50\ L/min$.

C. Experiment Setup and Assessment

The scheme proposed in section III is deployed for the RTO of the CSTR described previously. The kinetic parameters (k_1 and k_2) are assumed to be uncertain in the optimization model and they are bounded as $\boldsymbol{\Theta} = \{(k_1, k_2) | 0 < k_1, k_2 \leq 5\}$; in the plant, they manifest at their nominal values as stated in section IV*A*. All model states and the heat output are assumed to be measured $\boldsymbol{z} = [C_A \quad C_D \quad C_C \quad C_D \quad Q]^{\boldsymbol{T}}$ with a zero-mean additive Gaussian measurement noise of 0.1% the nominal measurement values (i.e., $\boldsymbol{w} \sim N(0, 0.001\boldsymbol{z_{nom}})$).

The RTO is run for 100 periods indexed as $l = \{0, \dots, T_f\}$. In each period, recurrent additive faults are inserted into randomly selected measurements with a magnitude sampled from a uniform distribution of $\pm 30\%$ the nominal measurement value (i.e., $f \sim 0.3U[-z_{nom}, z_{nom}]$). The fault locations and magnitudes do not vary within an RTO period as per assumption 3; however, they do vary with each new RTO period. $\alpha = 0.05$ is used for the bootstrapped GED scheme, which is deployed alongside a conventional RTO and compared in terms of mean parameter error (e_{θ_i}), sum of constraint violations (SAV), and mean process cost ($\bar{\phi}$), i.e.,

$$e_{\theta_i} = \frac{100\%}{T_f} \sum_{\forall l} \left| \hat{\theta}_i - \theta_{i,true} \right| \quad (16)$$

$$SAV = \frac{1}{T_f} \sum_{\forall l | g_i > g_{max}} (g_i - g_{max}) \quad (17)$$

$$\bar{\phi} = \frac{1}{T_f} \sum_{\forall l} \phi_l \quad (18)$$

The RTO sample size is $M = 50$ with a minimum number of measurements determined *a priori* as $n_{z,min} = 2$; given $n_z = 5$, this fulfills the criteria to deploy the proposed scheme as discussed in section III*C*. The computational experiments were performed on an Intel core i7-4770 CPU @ 3.4 GHz. The optimization problems and simulated plant were implemented in Pyomo [13] and the IPOPT solver [14] was used.

D. Single Fault Case

A single fault is first inserted into the measurements at every RTO interval. The summary metrics for this scenario applied to the CSTR as per (16)–(18) are shown in Table I (Single fault case). While the purity constraint (14) is inactive at the optimum, the safety constraint (13) is active and the cumulative constraint violations are an order of magnitude higher when not using the GED scheme as per the SAV. As the constraint being violated is a heating constraint, these excessively hot conditions can lead to equipment damage and potentially cause unsafe operation, e.g., injury to operators working closely with the CSTR. The reduction in violation is achieved through an 88% success rate in detecting faults when using the proposed GED framework. All faults not detected by the GED in this experiment were type II errors (false negatives). These occur as the parameter estimates generated using the faulty measurement were insufficiently erroneous as to not influence the estimate quality. The improvement in estimate quality is reflected in the reduced estimation error for both parameters (e_{k_1}, e_{k_2}) as shown in Table I; through these more accurate parameter estimates, the RTO produces points that violate constraint (13) less. The decreased constraint violation owed to the proposed method comes with no economic sacrifice as reflected in the mean costs ($\bar{\phi}$) in Table I where the prices of both schemes are the same. Indeed, in an active purity constraint case, abiding by the constraint could lead to higher product grade, thus better economics.

TABLE I. CSTR PERFORMANCE

	Single fault case		***Double fault case***	
Metric	***RTO***	***RTO+GED***	***RTO***	***RTO+GED***
$e_{k_1}(\%)$	8.75	1.55	8.11	1.38
$e_{k_2}(\%)$	9.60	4.90	4.57	1.24
$SAV(kcal/min)$	46.97	3.91	26.83	2.72
$\bar{\phi}$	15.27	15.27	15.41	15.41
# of faults inserted	–	100	–	200
# of faults correctly detected	–	88	–	160

Constraint violations are shown in Fig. 5, wherein cost contours are quantified with respect to the RTO-predicted optimal manipulated variable values. The RTO+GED scheme is observed to be less clustered in the constraint-violating region. Moreover, the standard RTO shows significant variance in its operation, with tails extending far into constraint violation. In cases where a constraint is violated, the RTO+GED scheme violates by a lesser amount than the conventional RTO. From the undetected faults, only one leads to a severe violation of the heating constraint as shown in Fig. 5 by the cyan point outside of the constraint boundary (this accounts for $2.12\ kcal/min$ of the SAV). The remaining eleven faults that the GED did not detect led to set points that were constraint-abiding or very close to the constraint boundary as per the remaining cyan points in Fig. 5. This is owed to the parameter-oriented testing approach introduced herein, which detects faults only if they are shown to propagate meaningfully to the parameters and resulting set points.

In terms of computational effort, each PE problem to be solved required an average of $0.015s$. For the CSTR system with $n_K(5,2) = 10$ parameter subsets and a sample size of $M = 50$; the mean bootstrapping computational effort was $7.5s$. This constitutes the main potential drawback of the proposed scheme: in systems with models that require high computational effort and have many measurements, the bootstrapped GED method may delay the RTO procedure, thus causing economic detriment.

E. Double Fault Case

Two faults are now inserted into the measurements simultaneously and the RTO+GED system must abate their effect. Table I summarizes the results for this scenario (Double fault case). A slightly lesser 80% success rate is observed in

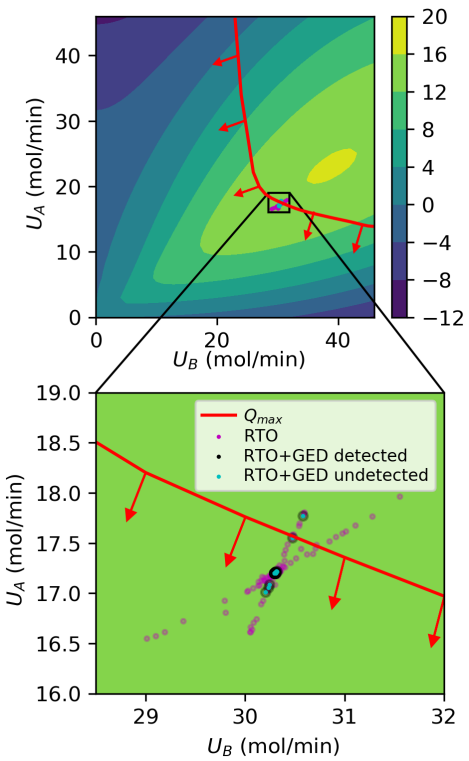

Figure 5. Single fault CSTR cost contours and RTO-generated operating points. Bottom pane magnified.

the two-fault case in terms of correctly identifying and eliminating errors whereby both errors were detected for 68% of RTO periods and a single error was detected for 24%. This minor deterioration in detection quality may occur as more measurements are removed from the original set as in the CSTR case. After removal of the first measurement, the new baseline has only four measurements, which can result in less averaging in $\bar{\boldsymbol{\theta}}$; thus, noisier estimates that allow for more random error to be admitted in the hypothesis tests. In cases with high performance deterioration, the critical significance level α could be tuned to admit more similar estimates.

Nonetheless, the decrease in success rate for detecting faults has little effect on performance as the difference between RTO and RTO+GED in the two-fault scenario is akin to that in the single-fault scenario in terms of the summary metrics in Table I. This is a result of using a parameter-oriented hypothesis test, which only detects faults if they have a significant effect on the estimate quality. Moreover, the CPU time for this case is the same as in the single fault case as computation does not scale with number of faults (i.e., the additional hypothesis testing cost is negligible with respect to the bootstrap).

V. Conclusion

A novel bootstrapped GED approach was proposed, which can be retrofitted into existing RTO-operated systems and leverages modern computational power. The scheme provides more accurate set points (i.e., closer to the true plant optima) than the traditional RTO method. In doing so, constraints are more frequently respected, which is particularly salient in settings where process safety constraints are considered. The proposed scheme is tested in a CSTR with a heat generation constraint whereby random faults are inserted into the measurements, the effect of which must be abated and identified. The GED+RTO is shown to provide order-of-magnitude improvement in constraint violation severity with respect to the traditional RTO procedure and demonstrates high accuracy in detecting faulty measurements. Moreover, this proposed scheme performs comparably in terms of process economics. This performance improvement is also observed in a two-fault case wherein a comparable detection rate was observed despite the presence of an additional fault.

The system tested in this work has few measurements and low computational burden, which allow for quick execution of the proposed algorithm. Future works will examine the performance of the scheme on systems with more measurements and more complex process models, wherein the computational effort of the scheme may be a limiting factor. On the other hand, more measurements will provide better averaging and truer parameter distributions with which to perform hypothesis testing, thus avoiding any deterioration caused by small sample sizes.

References

[1] M.L. Darby, M. Nikolaou, J. Jones, D. Nicholson, "RTO: An overview and assessment of current practice," *J. Process Control*, vol. 21, no. 6, pp. 874–884, Jul. 2011.

[2] N. Bizon, "Real-time optimization strategy for fuel cell hybrid power sources with load-following control of the fuel or air flow," *Energy Convers. Manag.,* vol. 157, 13–27, Feb. 2018.

[3] K.V. Pontes, I.J. Wolf, M. Embiruçu, W. Marquardt, "Dynamic Real-Time Optimization of Industrial Polymerization Processes with Fast Dynamics," *Ind. Eng. Chem. Res*., vol. 54, no. 47, pp. 11881–11893, Oct. 2015.

[4] G.D. Patrón, L. Ricardez-Sandoval, "An integrated real-time optimization, control, and estimation scheme for post-combustion CO_2 capture," *Appl. Energy*, vol. 308, 11830, Feb. 2022.

[5] J.F. Forbes, T.E. Marlin, "Model Accuracy for Economic Optimizing Controllers: The Bias Update Case," *Ind. Eng. Chem. Res*., vol. 33, no. 8, pp. 1919–1929, Aug. 1994.

[6] A.G. Marchetti, G. François, T. Faulwasser, D. Bonvin, "Modifier Adaptation for Real-Time Optimization—Methods and Applications," *Processes*, vol. 4, no. 4, 55, Dec. 2016.

[7] S.A. Bhat, D.N. Saraf, "Steady-State Identification, Gross Error Detection, and Data Reconciliation for Industrial Process Units," *Ind. Eng. Chem. Res*., vol. 43, no. 15, pp. 4323–4336, Jun. 2004.

[8] D.B. Özyurt, R.W. Pike, "Theory and practice of simultaneous data reconciliation and gross error detection for chemical processes," *Comput. Chem. Eng*., vol. 28, no. 3, pp. 381–402, Mar. 2004.

[9] I. Kim, M.S. Kang, S. Park, T.F. Edgar, "Robust data reconciliation and gross error detection: The modified MIMT using NLP," *Comput. Chem. Eng*., vol. 21, no. 7, pp. 775–782, Mar. 1997.

[10] M.A. Fischler, R.C. Bolles, "Random sample consensus: a paradigm for model fitting with applications to image analysis and automated cartography," *Commun. ACM*, vol. 24, no. 6, pp. 381–395, Jun. 1981.

[11] G.D. Patrón, L. Ricardez-Sandoval, "Low-Variance Parameter Estimation Approach for Real-Time Optimization of Noisy Process Systems," *Ind. Eng. Chem. Res*., vol. 61, no. 45, pp. 16780–16798, Nov. 2022.

[12] G. François, D. Bonvin, "Use of Transient Measurements for the Optimization of Steady-State Performance via Modifier Adaptation," *Ind. Eng. Chem. Res*., vol. 53, no. 13, pp. 5148–5150, Sept. 2013.

[13] W.E. Hart, J. Watson, D.L. Woodruff, "Pyomo: modeling and solving mathematical programs in Python," *Math. Program Comput.*, vol. 3, pp. 219–260, Aug. 2011.

[14] A. Wächter, L.T. Biegler, "On the implementation of an interior-point filter line-search algorithm for large-scale nonlinear programming," *Math. Program*., vol. 106, pp. 25−57, Apr. 2005.